ELSEVIER

Nuclear Physics A 624 (1997) 349–369

NUCLEAR PHYSICS A

Ground state properties of the β stable nuclei in various mean field theories ⋆

K. Pomorski [a,1], P. Ring [a], G.A. Lalazissis [a], A. Baran [b], Z. Łojewski [b], B. Nerlo-Pomorska [b], M. Warda [b]

[a] *Technische Universität München, Garching, Germany*

[b] *Katedra Fizyki Teoretycznej, Uniwersytet M.C.S., Lublin, Poland*

Received 12 March 1997; revised 1 May 1997

Abstract

The separation energies of neutrons and protons, binding energies, mean square charge radii, electric quadrupole moments and deformation parameters of the proton and neutron distributions are evaluated for β stable even–even nuclei with $16 \leqslant A \leqslant 256$. We compare the theoretical estimates obtained within the Hartree–Fock plus BCS model with a few sets of Skyrme forces, relativistic mean-field theory and frequently used Saxon–Woods and Nilsson potentials with experimental data. © 1997 Elsevier Science B.V.

PACS: 21.60.-n; 11.10.Ef; 21.10.-k; 21.30.Fe

1. Introduction

Mean field theory is a powerful tool for the description of low energy nuclear phenomena. Effective microscopic theories have been developed, the most fruitful being the Hartree–Fock calculations with effective density dependent interactions. Forces of Skyrme type [1,2] with zero range or of Gogny [3,4] type with finite range are among the most successful. In recent years a relativistic description of the ground state properties of nuclei has also been proposed. Relativistic mean field (RMF) theory [5] has been quite successful in describing finite nuclei at the line of β stability as well as far away from it [6,7].

⋆ This work is partly supported by the Polish Committee of Scientific Research under contract No. 2P03B 049 09.

[1] On leave on absence from the University M.C.S. in Lublin.

PII S0375-9474(96)00367-9

Apart from the microscopic effective theories, the macroscopic–microscopic models have also been developed. The Nilsson [8] and the Saxon–Woods [9] potentials have been widely used providing satisfactory results.

For the effective theories and the macroscopic–microscopic shell correction models mentioned above several parameter sets have been proposed. The number of the parameters varies in the different approaches. They are usually determined by a global fit to various ground state nuclear properties of β stable nuclei. The scope is always a better description of the available data and a hope to achieve in this way a higher predictive power for nuclei far away from stability.

The aim of this work is to analyze the results of several effective mean-field theories and of the shell correction models for the description of separation energies, sizes and shapes of neutron and proton distributions in the ground state of the β-stable even–even nuclei in a wide range of the mass numbers. The results are obtained using the most recent or frequently used parametrizations for each theory or model. This allows a systematic comparison of the different results of each theory close to β-stability. A reliable description of the nuclear ground state properties along the β-stability line is essential for a successful extrapolation to exotic nuclei as well as to superheavy nuclei. A similar comparison between results obtained with the SkIII and Ska Skyrme forces and the NL-1 and NL-2 sets of parameters of the RMF theory was done in Ref. [10]. Now, we are presenting results obtained with the Nilsson potential, five sets of the Saxon–Woods potential, eleven sets of the Skyrme forces and three sets of the RMF parameters.

In this paper we choose to investigate the Skyrme [1,2] mean field theory and the RMF [5] theory together with average potential models of Nilsson [8,11] and Saxon–Woods [12] type. The calculated quantities are the total binding energies (B), the proton (S_p) and neutron (S_n) separation energies, the mean square charge radii (MSR) and electric quadrupole moments (Q_2). The equilibrium deformations and root mean square radii (RMS) of proton and neutron distributions are also evaluated.

In Section 2 a brief discussion of the formalism used in each approach is presented. In Section 3 we give some details about the calculations and the observables under consideration. In Section 4 the results are presented and discussed. Finally in Section 5 the main conclusions are summarized.

2. The theoretical formalism

For a long time many results have been obtained by the macroscopic–microscopic model using phenomenological single-particle potentials. In the present investigation we have employed Nilsson and Saxon–Woods potentials. A short presentation of these models is given in Sections 2.1 and 2.2.

Hartree–Fock approach based upon phenomenological density dependent zero range forces of Skyrme type has proved to be very successful in the microscopic description of ground state properties of nuclear matter and of finite nuclei over the entire periodic table.

The Skyrme forces are presented in Section 2.3. In recent years relativistic mean field theory with nonlinear self-interactions between the mesons has gained in considerably interest for the investigations of low-energy phenomena in nuclear structure. With only a few phenomenological parameters such theories are able to give a quantitative description of ground state properties of spherical and deformed nuclei at the stability line and far away from it. In RMF theory the nucleons are described in a fully relativistic way as Dirac spinors interacting via the exchange of various mesons. In that sense the theory appears to be more fundamental since both nucleonic and mesonic degrees of freedom are taken into account. Moreover, the spin–orbit interaction is treated correctly and no extra parameter is necessary. In Section 2.4 we give a short description of the formalism of these theoretical approaches.

2.1. *The single-particle potential of Nilsson*

The modified anisotropic harmonic oscillator potential was introduced by Nilsson in Ref. [8] for the quadrupole deformation (ε) and a few years later it was generalized in Ref. [11] for deformations of higher multipolarity (ε_λ). The single particle hamiltonian with the Nilsson potential has the following form in the stretched coordinates system

$$\hat{H}_{\rm sp} = \frac{1}{2}\hbar\omega_0(\varepsilon,\varepsilon_4,\ldots)\left(-\Delta_\rho + \frac{1}{3}\varepsilon\left(2\frac{\partial^2}{\partial\zeta^2} - \frac{\partial^2}{\partial\xi^2} - \frac{\partial^2}{\partial\eta^2}\right)\right.$$
$$\left. +\rho^2\left[1 - \frac{2}{3}\varepsilon P_2(\cos\theta_t) + 2\varepsilon_4 P_4(\cos\theta_t) + \ldots\right]\right) + V_{\rm corr}. \tag{1}$$

where $\rho^2 = \xi^2 + \eta^2 + \zeta^2$ and the dimensionless stretched coordinates are defined as follows:

$$\xi = \sqrt{\frac{M\omega_\perp}{\hbar}}x, \qquad \eta = \sqrt{\frac{M\omega_\perp}{\hbar}}y, \qquad \zeta = \sqrt{\frac{M\omega_z}{\hbar}}z, \tag{2}$$

Here

$$\omega_\perp = \omega_0(\varepsilon,\varepsilon_4,\ldots)\left(1 + \frac{1}{3}\varepsilon\right) \quad \text{and} \quad \omega_z = \omega_0(\varepsilon,\varepsilon_4,\ldots)\left(1 - \frac{2}{3}\varepsilon\right). \tag{3}$$

The deformation dependence of the harmonic oscillator frequency ω_0 is obtained from the volume conservation condition

$$\frac{\omega_0^3}{\mathring{\omega}^3} = \frac{1}{\left(1+\frac{1}{3}\varepsilon\right)\left(1-\frac{2}{3}\varepsilon\right)^{1/2}}\int_0^1 \frac{d(\cos\theta_t)}{\left[1 - \frac{2}{3}\varepsilon P_2(\cos\theta_t) + 2\varepsilon_4 P_4(\cos\theta_t) + \ldots\right]^{3/2}}. \tag{4}$$

The frequency $\hbar\mathring{\omega}$ of the spherical harmonic oscillator was taken from Ref. [13]

$$\hbar\mathring{\omega} = 40/A^{1/3}\ \text{MeV}. \tag{5}$$

The correction potential $V_{\rm corr}$ in the Nilsson hamiltonian contains the spin–orbit (V_{ls}) and l^2 (V_{l^2}) terms

$$V_{\rm corr} = V_{ls} + V_{l^2}\,, \tag{6}$$

which were taken in the form proposed in Ref. [14]:

$$V_{ls} = -2\hbar\mathring{\omega}\kappa_{Nl}\boldsymbol{l}\cdot\boldsymbol{s}\,, \tag{7}$$

$$V_{l^2} = -\hbar\mathring{\omega}\left[\nu_{Nl}\boldsymbol{l}^2 - \langle\nu_{Nl}\boldsymbol{l}^2\rangle_N\right]. \tag{8}$$

The coeficients κ_{Nl} and ν_{Nl} are evaluated from the following expressions:

$$\kappa_{Nl} = \kappa_0\left[1 + 8\nu_{Nl}\left(N+\frac{3}{2}\right)\right] + \kappa_1 A^{-1/3}\int_{R_0-a/2}^{R_0+a/2}\mathcal{R}_{Nl}^2 r^2\,dr, \tag{9}$$

$$\nu_{Nl} = \nu_0\left[\int_0^{R_0-a/2}\mathcal{R}_{Nl}^2 r^2\,dr\right]^2, \tag{10}$$

where $R_0 = 1.2A^{1/3}$ fm is nuclear radius, $a = 0.7$ fm is the surface thickness and $\mathcal{R}_{Nl}(r)$ is the harmonic oscillator radial wave function. The correction term (6) in the Nilsson potential depends on three adjustable parameters only [14]:

$$\kappa_0 = 0.021, \qquad \kappa_1 = 0.90 \quad \text{and} \quad \nu_0 = 0.062, \tag{11}$$

which are valid in the all mass regions.

The potential energy of nucleus is calculated by the shell correction method [15] with the final range liquid drop (FRLD) macroscopic term [16] which contains also several fenomenological parameters.

2.2. *The single-particle potential of Saxon–Woods*

The deformed Saxon–Woods potential is widely described in the literature [12] and we restrict ourselves to represent only the basic formulae. The potential consists of the central part $V_{\rm cent}$, the spin–orbit part $V_{\rm so}$ and the Coulomb potential $V_{\rm Coul}$ for the protons:

$$V^{\rm WS}(\boldsymbol{r},\boldsymbol{p},\boldsymbol{s};\beta) = V_{\rm cent}(\boldsymbol{r};\beta) + V_{\rm so}(\boldsymbol{r},\boldsymbol{p},\boldsymbol{s};\beta) + V_{\rm Coul}(\boldsymbol{r};\beta)\,, \tag{12}$$

with

$$V_{\rm so}(\boldsymbol{r},\boldsymbol{p},\boldsymbol{s};\beta) = -\lambda(\nabla V_{\rm cent}\times\boldsymbol{p})\cdot\boldsymbol{s}\,. \tag{13}$$

The central part is defined by:

$$V_{\rm cent}(\boldsymbol{r};\beta) = \frac{V_0[1 \overset{+}{-} \kappa(N-Z)/A]}{[1+\exp(l(\boldsymbol{r};\beta)/a)]}\,, \tag{14}$$

where a is the diffuseness of the nuclear surface. The set of deformation parameters β_λ, which characterize the nuclear shape, is denoted by β. The function $l(\boldsymbol{r},\beta)$, describing

Table 1
Different sets of parameters of the Saxon–Woods potential (Eq. (12)). "universal" [12], Wahlborn [9], Rost [17], Chepurnov [18] and the "new" [19] ones were chosen

Parameter	Units	Universal	Wahlborn	Rost	Chepurnov	New
V_0	MeV	49.6	51.0	49.6	53.3	49.6
κ	–	0.86	0.67	0.86	0.63	0.86
a	fm	0.70	0.67	0.70	0.63	0.70
r_n	fm	1.347	1.27	1.347	1.24	1.347
λ_n	–	35.0	32.0	31.5	$23.8 \times (1+2I)$	[a]
r_n^{so}	fm	1.31	1.27	1.280	1.24	[a]
r_p	fm	1.275	1.27	1.275	1.24	1.275
λ_p	–	36.0	32.0	17.8	$23.8 \times (1+2I)$	[a]
r_p^{so}	fm	1.32	1.27	0.932	1.24	[a]

[a] The radius constant and the strenght of the spin–orbit potential are deformation dependent as described in Ref. [19].

the distance between the given point $\boldsymbol{r}$ and the nuclear surface has been determined numerically [12]. For spherical nuclei we have $l(\boldsymbol{r}, \beta = 0) = r - R_0$, where $R_0 = r_0 A^{1/3}$, is the radius of the corresponding spherical nucleus.

$$R(\theta) = c(\beta) R_0 \left[1 + \sum_{\lambda} \beta_\lambda Y_{\lambda 0}(\cos(\theta)) \right] . \tag{15}$$

The function $c(\beta)$ insures the conservation of the nuclear volume with a change of the nuclear shape.

The various sets of Saxon–Woods potential parameters are presented in Table 1. The "universal" [12], Wahlborn [9], Rost [17], Chepurnov [18] and the "new" [19] ones were chosen.

2.3. *Effective mean field theory with Skyrme forces*

Mean field theory of the Skyrme type starts from an energy functional, which is derived from a density dependent two-body interaction of the form:

$$\begin{aligned} V_{12} = {} & t_0(1 + x_0 P_\sigma)\, \delta(\boldsymbol{r}_1 - \boldsymbol{r}_2) \\ & -\frac{1}{2} t_1 (1 + x_1 P_\sigma) \left[\overleftarrow{\nabla}_{12}^2 \delta(\boldsymbol{r}_1 - \boldsymbol{r}_2) + \delta(\boldsymbol{r}_1 - \boldsymbol{r}_2) \overrightarrow{\nabla}_{12}^2 \right] \\ & -t_2 (1 + x_2 P_\sigma) \overleftarrow{\nabla}_{12} \delta(\boldsymbol{r}_1 - \boldsymbol{r}_2) \overrightarrow{\nabla}_{12} \\ & +\frac{1}{6} t_3 (1 + x_3 P_\sigma) \left[\rho_{q_1}(\boldsymbol{r}_1) + \rho_{q_2}(\boldsymbol{r}_2) \right]^\gamma \delta(\boldsymbol{r}_1 - \boldsymbol{r}_2) \\ & -i\omega_0 \overleftarrow{\nabla}_{12} \wedge \delta(\boldsymbol{r}_1 - \boldsymbol{r}_2) \overrightarrow{\nabla}_{12} \cdot (\boldsymbol{\sigma}_1 + \boldsymbol{\sigma}_2) + V_{\text{Coul}} , \end{aligned} \tag{16}$$

where $t_0, t_1, t_2, t_3, x_1, x_2, x_3, w_0$ and γ parameters are shown in Table 2 as 10 sets called: *i* [2], *ii* [20], *iii*, *iv*, *v*, *vi* [21], *vii* [22], $m^\star$ [23], *a* [24], *p* [25]. P_σ is the spin exchange operator.

Table 2
Parameters of the Skyrme forces (Eq. (16)) used in our calculations. *i* [2], *ii* [20], *iii*, *iv*, *v*, *vi* [21], *vii* [22], m^* [23], *a* [24], *p* [25]

Parameter	Unit	*i*	*ii*	*iii*	*iv*	*v*
t_0	MeV fm^3	−1057.30	−1057.30	−1128.75	−1205.60	−1248.29
t_1	MeV fm^5	235.90	235.90	395.00	765.00	970.56
t_2	MeV fm^5	−100.00	−100.00	−95.00	35.00	107.22
t_3	MeV fm$^{(3+3\gamma)}$	14463.5	14463.5	14000.0	5000.0	0.0
x_0	–	0.560	0.560	0.450	0.050	−0.170
x_1	–	0	0	0	0	0
x_2	–	0	0	0	0	0
x_3	–	0	0	0	0	0
γ	–	1	1	1	1	1
w_0	MeV fm^5	120.0	105.0	120.0	150.0	150.0

Parameter	Unit	*vi*	*vii*	*p*	m^*	*a*
t_0	MeV fm^3	−1101.81	−1096.00	−2931.70	−2645.00	−1602.78
t_1	MeV fm^5	271.67	246.20	320.62	410.00	570.88
t_2	MeV fm^5	−138.33	−148.00	−337.41	−135.00	−67.70
t_3	MeV fm$^{(3+3\gamma)}$	17000.0	17626.0	18708.97	15595.0	8000.0
x_0	–	0.583	0.620	0.29215	0.090	−0.020
x_1	–	0	0	0.65318	0	0
x_2	–	0	0	−0.53732	0	0
x_3	–	0	1	0.18103	0	0.286
γ	–	1	1	$\frac{1}{6}$	$\frac{1}{6}$	$\frac{1}{3}$
w_0	MeV fm^5	115.0	112.0	100.0	130.0	125.0

Using Slater determinants as variational functions the energy functional of a nucleus can be expressed as a volume integral:

$$E = \int H(\boldsymbol{r})\, d^3\boldsymbol{r}\ , \tag{17}$$

where the energy density $H(\boldsymbol{r})$ is a function of the nucleon density ρ, the kinetic energy density τ and spin density $\boldsymbol{J}$. The total energy (17) has to be minimized with respect to the choice of the many-body wave functions, which leads to a nonlinear eigenproblem with the corresponding mean-field hamiltonian.

2.4. The relativistic Hartree formalism

RMF theory is based on an effective lagrangian containing both nucleonic and mesonic degrees of freedom [5,26]:

$$\begin{aligned}\mathcal{L} = {} & \bar{\psi}_i\{i\gamma^\mu\partial_\mu - M\}\psi_i \\ & + \frac{1}{2}\partial^\mu\sigma\,\partial_\mu\sigma - U(\sigma) - g_\sigma\bar{\psi}_i\psi_i\,\sigma \\ & - \frac{1}{4}\Omega^{\mu\nu}\Omega_{\mu\nu} + \frac{1}{2}m_\omega^2\,\omega^\mu\omega_\mu - g_\omega\bar{\psi}_i\,\gamma^\mu\,\psi_i\,\omega_\mu\end{aligned} \tag{18}$$

Table 3
Parameters used in the relativistic mean-field lagrangian, Eq. (19). NL-1 [28], NL-SH [29], NL-3 [27]

Parameter	Units	NL-1	NL-SH	NL-3
M	MeV	938.0	939.0	939.0
m_σ	MeV	492.25	526.059	508.194
m_ω	MeV	795.359	783.00	782.501
m_ρ	MeV	763.000	763.00	763.000
g_σ	-	10.138	10.4444	10.217
g_2	fm^{-1}	−12.172	−6.9099	−10.431
g_3	-	−36.265	−15.8337	−28.885
g_ω	-	13.285	12.945	12.868
g_ρ	-	4.976	4.383	4.474

$$-\frac{1}{4}\boldsymbol{R}^{\mu\nu}\boldsymbol{R}_{\mu\nu}+\frac{1}{2}m_\rho^2\,\boldsymbol{\rho}^\mu\boldsymbol{\rho}_\mu-g_\rho\bar{\psi}_i\,\gamma^\mu\boldsymbol{\tau}\,\psi_i\,\boldsymbol{\rho}_\mu$$
$$-\frac{1}{4}F^{\mu\nu}F_{\mu\nu}-e\bar{\psi}_i\,\gamma^\mu\,\frac{(1-\tau_3)}{2}\,\psi_i\,A_\mu,$$

where M is the nucleon mass, $m_\sigma, m_\omega, m_\rho$ are meson masses, and $g_\sigma, g_\omega, g_\rho$ are meson coupling constants. The isovector quantities are indicated by arrow bars. In our approach we use the nonlinear σ–ω–ρ model, that is we consider that the sigma mesons move in their nonlinear potential created by the other ones:

$$U(\sigma)=\frac{1}{2}m_\sigma^2\sigma^2+\frac{1}{3}g_2\sigma^3+\frac{1}{4}g_3\sigma^4. \tag{19}$$

The parameters of RMF theory are gathered in Table 3: NL-1 [28], NL-3 [27], NL-SH [29].

The classical variational principle yields a coupled set of equations of motion for the Dirac spinors and the fields: the Dirac equation for the nucleons, Klein–Gordon equations for the meson fields and the Laplace equation for the Coulomb field. The solution of this nonlinear set of coupled equations is carried out iteratively. The calculations for both the Skyrme mean field as well as the RMF theory have been carried out in the axial symmetric configuration using the oscillator expansion method [30].

3. Details of the calculations

Since most of the nuclei considered here are open shell nuclei, pairing has been included using the BCS formalism. We have used constant pairing gaps for protons and neutrons which have been obtained from the empirical particle separation energies by the formulae:

$$\Delta_{\mathrm{p}}(Z,N)=\frac{1}{4}\left(B(Z-2,N)-3B(Z-1,N)+3B(Z,N)-B(Z+1,N)\right), \tag{20}$$

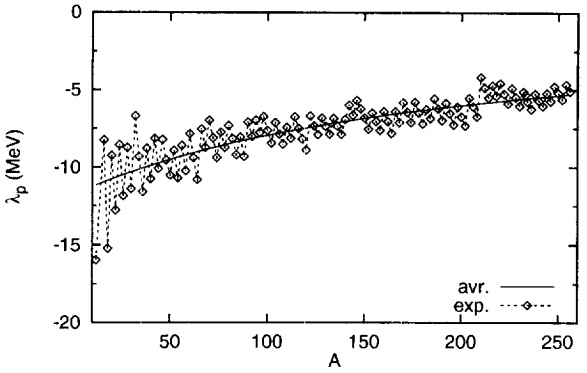

Fig. 1. The estimated "experimental" position of the proton Fermi levels (diamonds, "exp.") for even–even nuclei along the β-stability line. The solid line (avr.) was obtained from the phenomenological formula (24)–(25).

$$\Delta_n(Z,N) = \frac{1}{4}\left(B(Z,N-2) - 3B(Z,N-1) + 3B(Z,N) - B(Z,N+1)\right). \tag{21}$$

The calculations were performed for the pairing window consisting of Z (or N) lowest single particle levels for protons (or neutrons).

It should be noted that for constant pairing gaps $\Delta_{n(p)}$ the pairing energy diverges if it is extended over an infinite configuration space. Therefore in all of our calculations a pairing window has been considered.

We have chosen nuclei with the smallest mass for a given nucleon number A. Obviously these nuclei are stable against β-decay. We have considered in our analysis the even–even nuclei with $16 \leqslant A \leqslant 256$. For all these nuclei calculations for the total binding energy have been carried out.

For an estimate of the proton (neutron) separation energies an approximate method is proposed. It is known from the BCS theory that in order to separate a nucleon from an even–even nucleus one has to break the Cooper pair and to move this nucleon from the Fermi level (λ) to the continuum limit. This experimental relation can be written as follows:

$$\lambda_p(Z,N) = \Delta_p(Z,N) - S_p(Z,N), \tag{22}$$

$$\lambda_n(Z,N) = \Delta_n(Z,N) - S_n(Z,N). \tag{23}$$

The values of these "experimental" Fermi energies (exp, diamonds) are plotted in Figs. 1 and 2 for protons and neutrons respectively. The solid lines (avr) in Figs. 1 and 2 correspond to the average position of the Fermi level obtained by the phenomenological formula:

$$\bar{\lambda}_p = \frac{-11.8\ \text{MeV}}{1 + A/208}, \tag{24}$$

$$\bar{\lambda}_n = \bar{\lambda}_p - 0.512\ \text{MeV}. \tag{25}$$

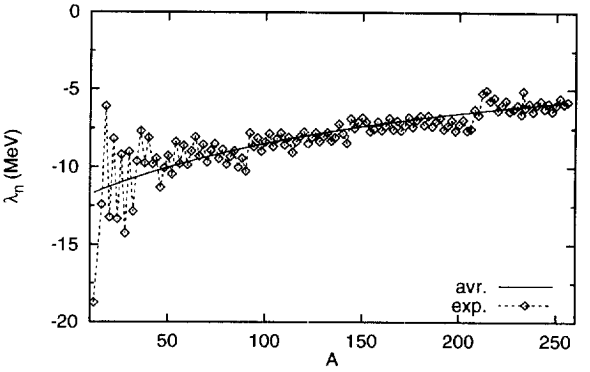

Fig. 2. The same as in Fig. 1 but for neutrons.

The coefficients in Eqs. (24) and (25) were obtained by the least square fit to the experimental values of the Fermi energies of all β-stable nuclei. The average position of the Fermi level for neutrons is shifted down with respect to the Fermi level for protons by one electron mass as one would expect from general thermodynamical considerations.

The values of $\bar{\lambda}_p$ and $\bar{\lambda}_n$ [31] as well as the average MSR radii of nuclei [32] can be used to establish the depth and size of the average potential well for β-stable nuclei.

We are interested in quantities characterizing the neutron and proton distribution in nuclei, their sizes and shapes. Thus, we have performed systematic calculations of the proton and neutron mean square radii and of the proton and neutron deformation parameters $\beta_{n(p)}$.

The charge radii were calculated from the corresponding proton radii taking into account the correction due to finite proton size:

$$\langle r^2\rangle_{ch} = \langle r^2\rangle_p + 0.64\ \mathrm{fm}^2. \tag{26}$$

Here we have neglected the small contributions to the mean charge square radius originating from the electric neutron form factor and the electromagnetic spin–orbit coupling [33,34] as well as the corrections due to the center of mass motion.

The global measure of the deformation of the neutron (or proton) distribution in the case of the microscopic theories can be expressed by the corresponding quadrupole moment

$$\langle Q_2\rangle_{n,p} = \langle 2r^2 P_2(\cos\theta)\rangle\,. \tag{27}$$

Having the quadrupole and monopole moments we can estimate approximately the quadrupole deformation parameter β of the neutron (or proton) distribution [35]

$$\beta_{n,p} = \sqrt{\frac{\pi}{5}}\frac{\langle Q_2\rangle_{n,p}}{\langle Q_0\rangle_{n,p}}\,, \tag{28}$$

where $\langle Q_0\rangle_n = N\langle r^2\rangle_n$ and $\langle Q_0\rangle_p = Z\langle r^2\rangle_p$. This simple estimate for the quadrupole deformation is valid only for small deformation parameters β.

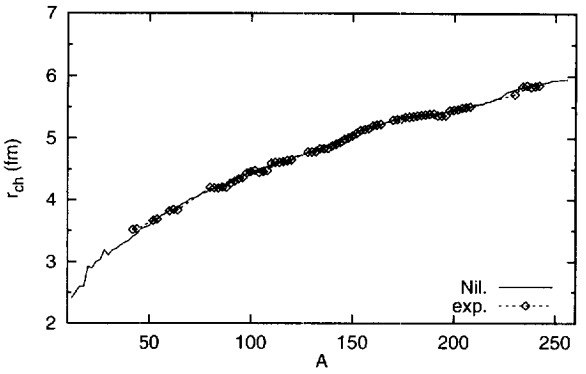

Fig. 3. The charge root mean square radii obtained with the Nilsson potential (solid line, "Nil.") are compared with the experimental data [36,37] (diamonds, "exp.").

The reduced electric quadrupole transition between the rotational 2^+ and 0^+ states are proportional to the square of the proton quadrupole moment

$$B(\mathrm{E2}) = \frac{5}{4\pi}\langle Q_2\rangle_{\mathrm{p}}^2. \tag{29}$$

4. Numerical results and discussion

4.1. Macroscopic–microscopic models

Using the single-particle Nilsson potential and the well known Strutinsky [15] shell correction method with the renormalisation to the finite range liquid droplet model [16] we have found the ground state deformations of all the investigated nuclei. We are not going to compare here the total binding energy of a nucleus with the experimental data because this observable is not only dependent on the potential but also on the macroscopic part. We know from the extended calculations made e.g. in Ref. [16] that the advanced macroscopic–microscopic model leads to very good estimates of the nuclear masses much closer to the experimental data than those obtained within the microscopic theories. One should keep in mind, however, the large number of parameters of these models as well as the large experimental input used for their determination.

Having the ground state deformations we have evaluated microscopically the mean square charge radii (MSR) and the reduced electric quadrupole transition probabilities (B(E2)) in the corresponding equilibrium points. The Nilsson model estimates of the radii r_{ch} are plotted in Fig. 3 and of B(E2)-values in Fig. 4. The theoretical results are compared with the experimental data taken from Refs. [36,37]. It is seen in Fig. 3 that the Nilsson average potential reproduces very well the experimental trend of r_{ch} in the whole range of A. The mean square deviation of the theoretical values from the experimental data is

$$\langle \Delta^2 r_{\mathrm{ch}}\rangle^{1/2} = 0.029 \text{ fm}. \tag{30}$$

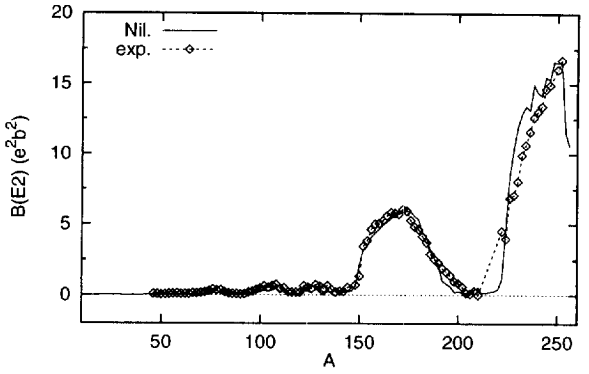

Fig. 4. The reduced transition probabilities B(E2) obtained with the Nilsson potential (solid line, "Nil.") compared with the experimental data (diamonds, "exp.") [37].

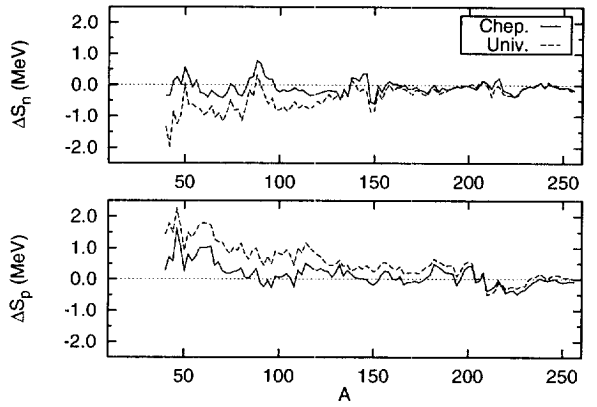

Fig. 5. The differences between the theoretical and experimental [31] separation energies of protons S_p and neutrons S_n. The theoretical estimates were obtained with the Saxon–Woods potential with the Chepurnov [18] parameters set (solid line, "Chep.") and universal set [12] (dashed line, "Univ.").

The calculated $B(E2)$ transition probabilities are also close to the experimental values:

$$\langle \Delta^2 B(E2) \rangle^{1/2} = 1.336\ e^2b^2. \tag{31}$$

Only in the region of $A \approx 220$ are our estimates of $B(E2)$ too large. It is probably due to the lack of octupole deformation of these heavy nuclei in our analysis. We have performed the calculations with the Nilsson potential for one set of the correction term parameters [14] valid in the whole range of A [38].

The infinite Nilsson potential is not adjusted for reproducing the separation energies of the neutron (S_n) or of the proton (S_p). We can easily obtain such estimates with the Saxon–Woods potential and we have performed an extensive calculation for five commonly used sets of parameters (see Table 1). The results are presented in Fig. 5, where the differences between the theoretical and the experimental [31] separation energies of protons and neutrons are plotted. The best theoretical estimates of S_n and S_p were obtained with the Saxon–Woods potential of Chepurnov [18]. For the sake

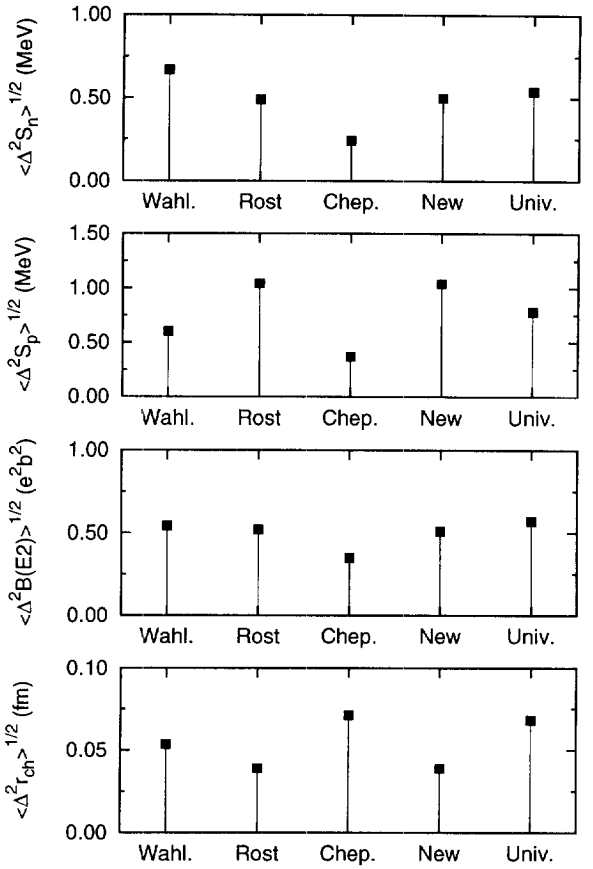

Fig. 6. The root mean square errors for the neutron (S_n) and proton (S_p) separation energies, the reduced transition probabilities $B(E2)$ and the charge radii (r_{ch}) obtained within different Saxon–Woods potentials (Table 1).

of comparison we present also the results for the commonly used "universal" set of parameters [12] (Fig. 5).

The mean square deviations between the theoretical and experimental values of S_n, S_p, $B(E2)$ and r_{ch} for all investigated Saxon–Woods models are plotted in Fig. 6. It is seen that the Chepurnov set apart from the charge radii gives the smallest deviations from the experiment. For the charge radii r_{ch} the other sets are somewhat better than Chepurnov parametrization.

4.2. *Self-consistent theories*

A similar analysis of the β-stable even–even nuclei features has also been performed within the Hartree–Fock model with density dependent Skyrme forces as well as within the RMF theory.

The root mean square errors for the neutron (S_n) and proton (S_p) separation energies,

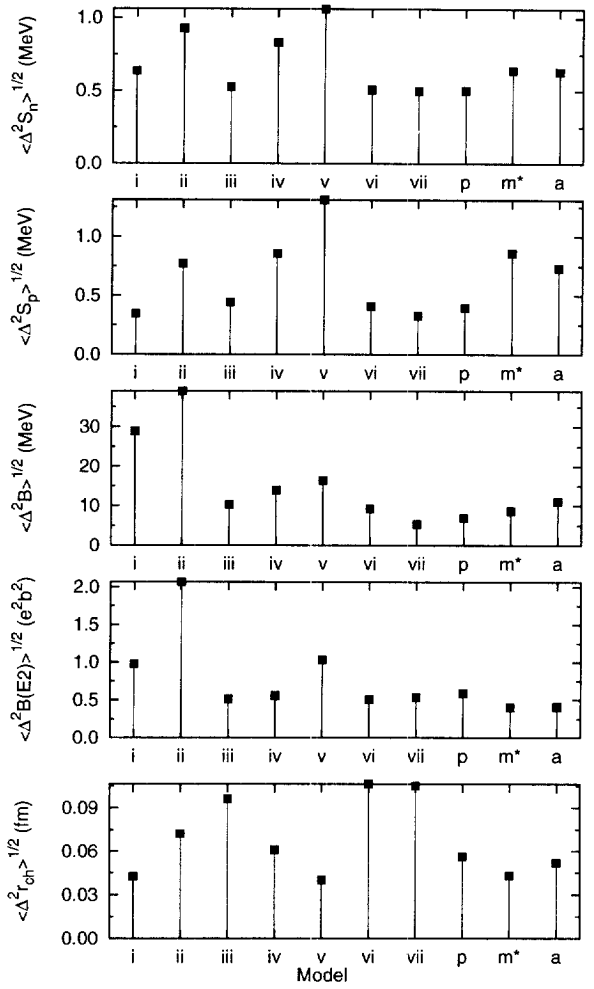

Fig. 7. The root mean square errors for the neutron (S_n) and proton (S_p) separation energies, the binding energies (B), the reduced transition probabilities B(E2) and charge radii (r_{ch}) obtained within the HFB calculation for different sets of the Skyrme forces (Table 2).

the binding energies per particle (B), the reduced transition probabilities (B(E2)) and charge radii (r_{ch}) were obtained within the HF+BCS scheme for ten different sets of the Skyrme forces (see Table 2). These mean square deviations are plotted in Fig. 7. It is seen that on the average the predictions of m^* and p effective forces are closest to the experiment. It is noted however, that the other sets give also quite reasonable predictions for certain observables.

We have also investigated the deviation of the calculated quantities from those of the empirical values as a function of the mass number. This is given in Fig. 8 for the parameter sets *iii*, p and m^*. One cannot draw a firm conclusion as to which set is better. It should be noted, however, that the predictions of m^* for the B(E2) transitions

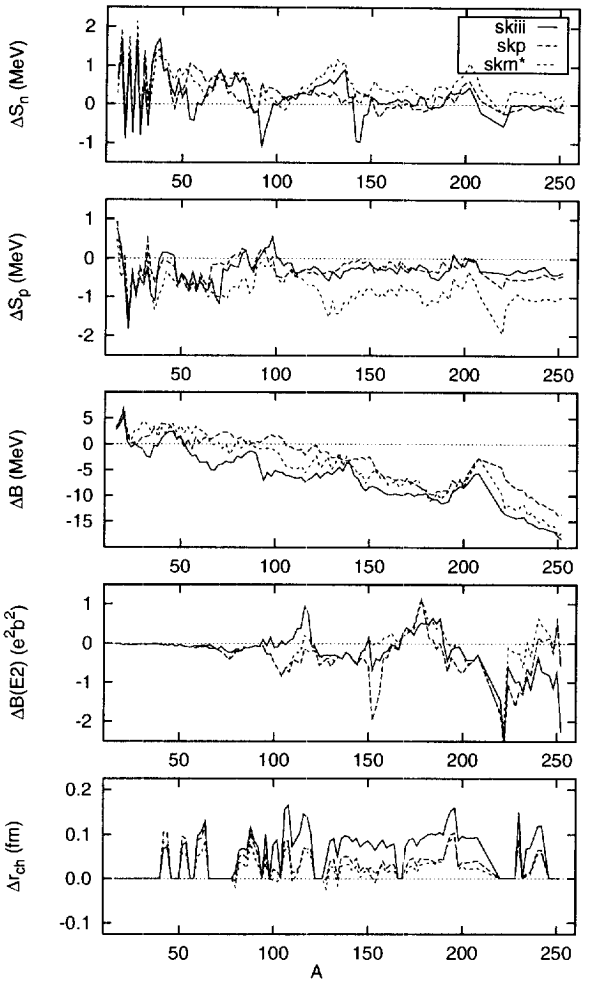

Fig. 8. The differences between the theoretical and experimental [31] separation energies of neutrons (S_n) and protons (S_p), the binding energies (B), the reduced transition probabilities B(E2) and the charge radii (r_{ch}) for the nuclei along the β-stability line. The theoretical estimates were obtained within the HFB calculation for *iii*, *p* and m^* sets of the Skyrme forces (Table 2).

and the charge radii seem to be much closer to the empirical values than those for the other forces.

In Fig. 9 the neutron skin thickness (r_n–r_p) is plotted against mass number A for the same three Skyrme sets. It is seen that for the iii set the smallest neutron skin thickness appears. The other two sets give similar results of the difference in radii not exceeding 0.15 fm. Finally in Fig. 10 the differences (β_n–β_p) of the neutron and proton deformation parameters are shown. It is seen that the difference increases with the mass number. It is also seen that for heavier nuclei the proton distribution appears to be more deformed than the neutron distribution as was already noticed in Refs. [39,40].

A similar procedure was also followed for the RMF theory. In this case the parameter

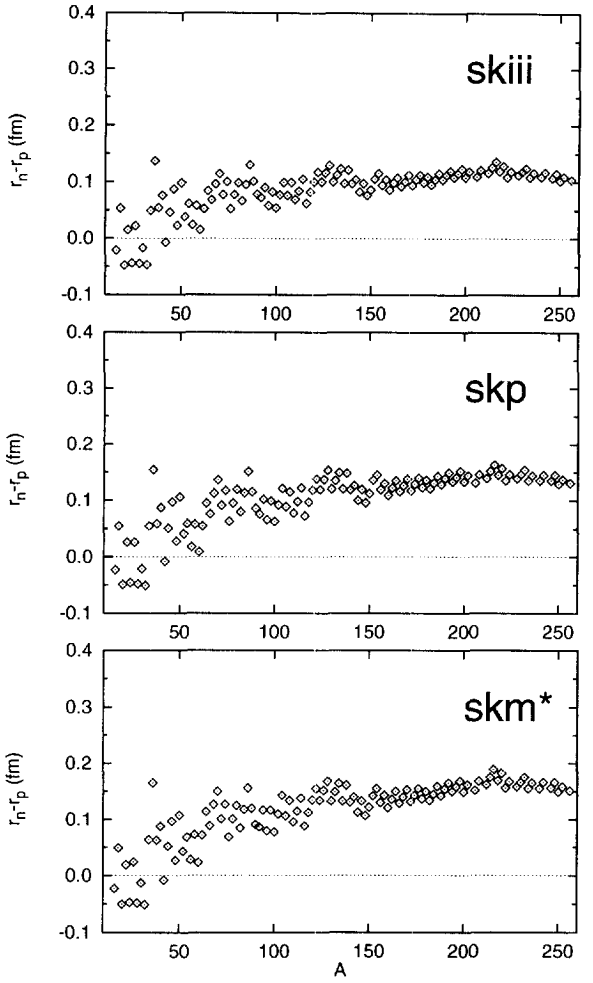

Fig. 9. The differences (diamonds) between the mean square radii of the neutron (r_n) and proton (r_p) density distributions evaluated within the HFB calculation with the *iii*, *p* and m^* Skyrme forces (Table 2) for the nuclei along the β-stability line.

sets NL-1, NL-3, NL-SH (see Table 3) were employed.

In Fig. 11 the mean square deviations for the various observables calculated with the three parameter sets are shown. It is seen that all sets give satisfactory results with NL-3 and NL-SH being slightly better. In Fig. 12 the differences of the calculated values from the experimental ones are given as functions of the mass number. Especially the masses are reproduced much better with NL-3. In Figs. 13 and 14 the neutron skin and the difference of the proton neutron deformation parameters are plotted against mass number A. The behaviour is rather similar in all parametrizations. For NL-1 the neutron skin is larger than in the other two forces. This could be attributed to the large asymmetry energy of NL-1. The differences of the proton neutron deformation parameters show rather similar behaviour in all sets [39,40].

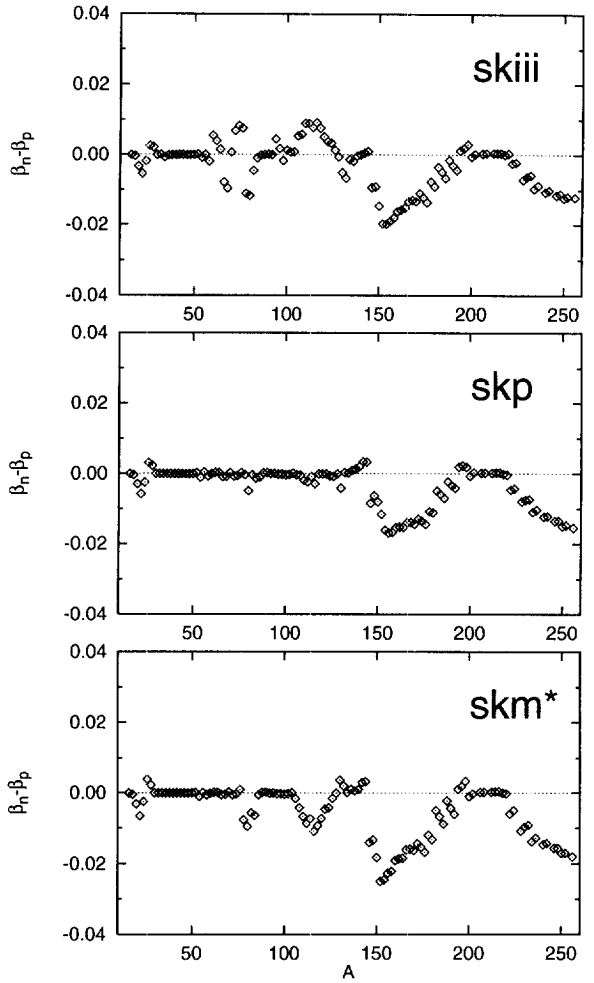

Fig. 10. The difference (diamonds) between the quadrupole deformation of the neutron (β_n) and proton (β_p) density distributions obtained within the HFB calculation with the *iii*, *p* and m^* Skyrme forces (Table 2) for the nuclei along the β-stability line.

5. Conclusions

In this work a systematic study of the ground state properties of β stable nuclei has been performed within various effective microscopic theories and potential models. Best parametrizations among the most frequently used have been employed for each theoretical approach. The aim was an investigation of the behaviour of the various parameter sets over a wide range of mass numbers.

The best estimates of the mean square charge radii for the β-stable nuclei are obtained with the Nilsson potential with the parameters taken from Ref. [14]. It turned out that the Chepurnov [18] parametrization gives on the average the best results among the considered parameter sets of the Saxon–Woods potential.

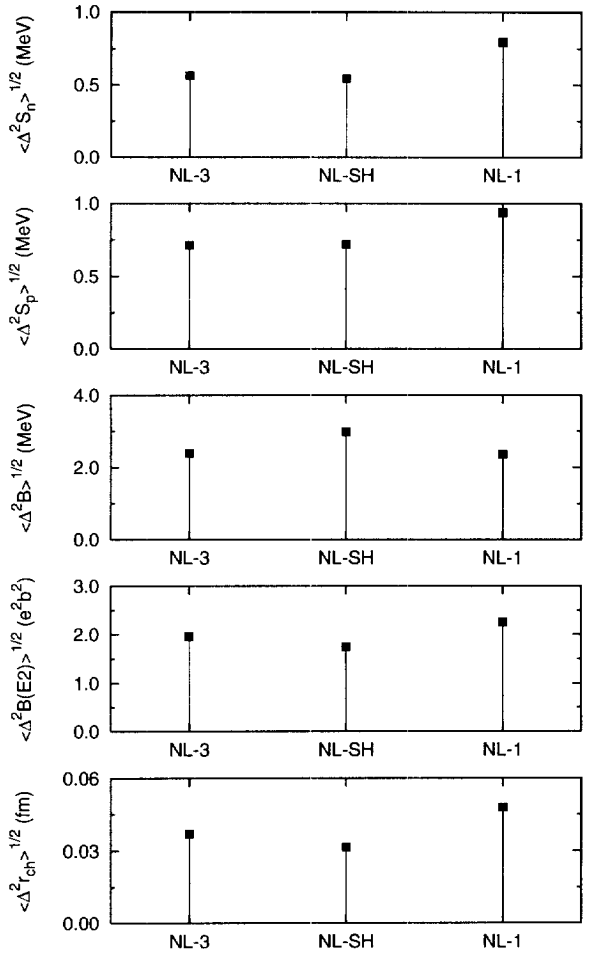

Fig. 11. The same as in Fig. 7 but for the estimated obtained within the RMF theory for NL-3, NL-SH and NL-1 sets of parameters (Table 3).

For Skyrme theory the effective forces m^* [23] and p [25] seem to give the most satisfactory results for the calculated observables.

In RMF theory the lagrangian parametrizations NL-1, NL-3 and NL-SH have been considered. The study showed that along β stability line all sets work well with the NL-3 [27] force being somewhat better, especially in the binding energy predictions.

A few more comments are in place:

(i) In the microscopic theories (Skyrme or RMF) the neutron skin for the β-stable nuclei grows with A. In the Skyrme mean field the neutron mean square radii are larger than the proton ones by 0.15 fm for the heaviest isotopes. In the RMF theory the neutron skin is somewhat larger, being about 0.25 fm.

(ii) Both Skyrme mean field and RMF present a significant difference in the quadrupole deformation of the neutron and proton distributions, the protons distribution being

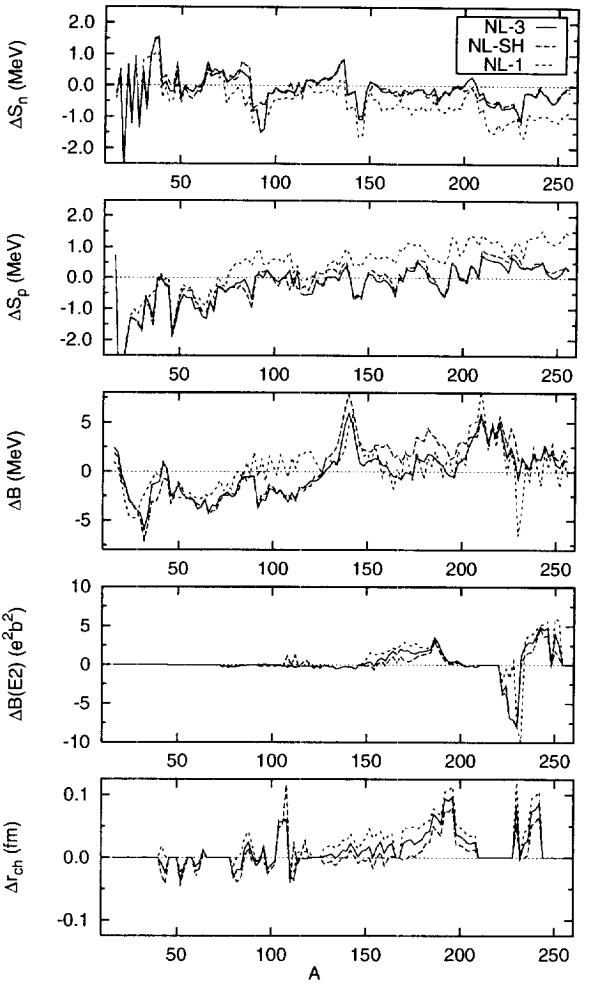

Fig. 12. The same as in Fig. 8 but for the estimates obtained within the RMF theory for NL-3, NL-SH and NL-1 sets of parameters (Table 3).

more deformed than the neutrons one. This difference can become larger than 10% of the total magnitude of the deformation.

(iii) These two effects should be taken into account in the macroscopic–microscopic models, e.g. in the liquid droplet model plus the Strutinsky shell correction for the Saxon–Woods or Nilsson single particle levels. The effect of the different deformations of the proton and neutron distribution can be also important for the calculation of the fission barriers using potential models. This was already suggested in Ref. [39,40].

The different density distributions of protons and neutrons in a nucleus should be taken into account in all the calculations where the collective variables enter parametrically in order to minimize the potential energy of the nucleus. We think that it would be

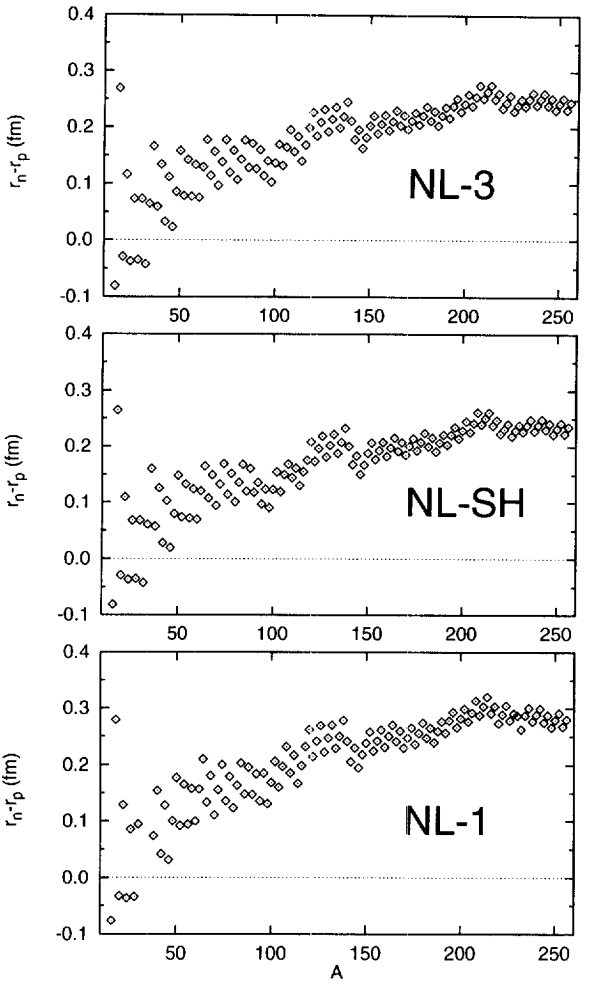

Fig. 13. The same as in Fig. 9 but for the estimates obtained within the RMF theory for NL-3, NL-SH and NL-1 sets of parameters (Table 3).

worthwhile to look at proton and neutron equilibrium deformation separately in the macroscopic–microscopic type of calculations.

Acknowledgements

Krzysztof Pomorski gratefully acknowledges the warm hospitality extended to him by the Theoretical Physics Group of the Technical University in München as well as a grant from the Deutsche Forschung Gemeinschaft. Another author (G.A.L) acknowledges the warm hospitality of the theory group of the Maria Curie Skłodowska University during his short stay in Lublin, and financial support by the E.U. under the contract TMB-EU/ERB FMBCICT-950216. The authors thank Professor Klaus Dietrich of TUM for helpful discussions.

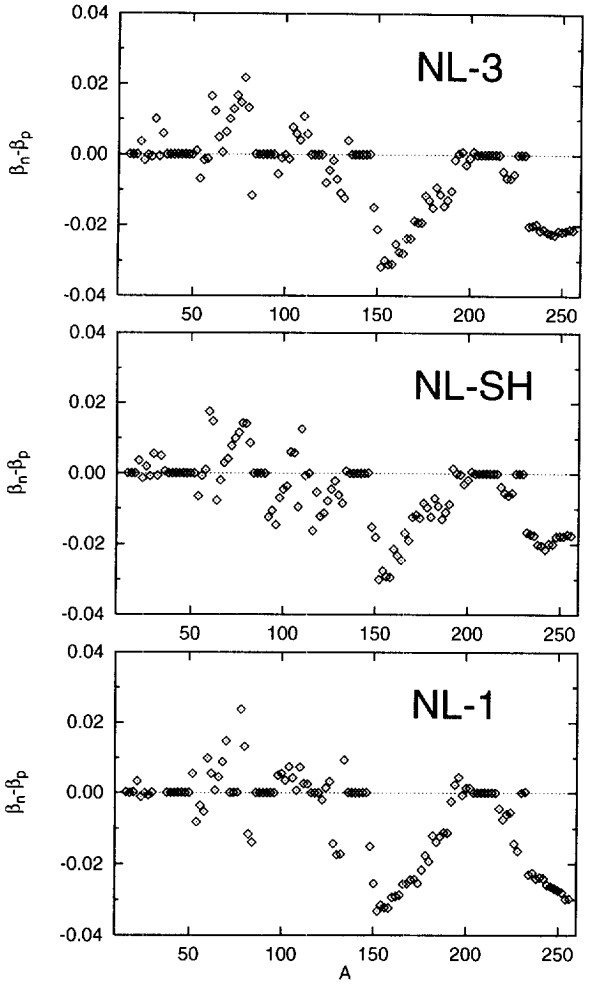

Fig. 14. The same as in Fig. 10 but for the estimates obtained within the RMF theory for NL-3, NL-SH and NL-1 sets of parameters (Table 3).

References

[1] T.H.R. Skyrme, Phil. Mag. 1 (1956) 1043; Nucl. Phys. 9 (1958) 615.
[2] D. Vautherin and D.M. Brink, Phys. Rev. C 5 (1972) 626;
H. Flocard, P. Quentin, A.K. Kerman and D. Vautherin, Nucl. Phys. 203 (1973) 3.
[3] D. Gogny, Nuclear Self-Consistent Fields, ed. G. Ripka and M. Porneuf (North Holland, 1975).
[4] J.F. Berger, M. Girod and D. Gogny, Nucl. Phys. A 428 (1984) 23c.
[5] B.D. Serot and J.D. Walecka, The Relativistic Nuclear Many-Body Problem, *in* Advances in Nucl. Phys., ed. J.W. Negele and Erich Vogt, Vol. 16 (Plenum, New York, 1986).
[6] D. Hirata, H. Toki, T. Watabe, I. Tanihata and B.V. Carlson, Phys. Rev. C 44 (1991) 1467.
[7] W. Koepf, Y.K. Gambir, P. Ring and M.M. Sharma, Z. Phys. A 340 (1991) 119.
[8] S.G. Nilsson, Mat. Fys. Medd. Dan. Vid. Selsk. 29 No. 16 (1955).
[9] J. Blomquist and S. Wahlborn, Ark. Fiz. 16 (1960) 543.
[10] K. Sumiyoshi, D. Hirata, H. Toki and H. Sagawa, Nucl. Phys. A 552 (1993) 437.
[11] C. Gustafson, I.L. Lamm, B. Nilsson and S.G. Nilsson, Ark. Phys. 36 (1967) 613.

[12] S. Ćwiok, J. Dudek, W. Nazarewicz, J. Skalski and T. Werner, Comp. Phys. Comm. 46 (1987) 379.
[13] B. Nerlo-Pomorska, K. Pomorski and B. Skorupska-Mach, Nucl. Phys. A 562 (1993) 80.
[14] T. Seo, Z. Phys. A 324 (1986) 43.
[15] V.M. Strutinsky, Yad. Fiz. 3 (1966) 614.
[16] P. Möller, J.R. Nix, W.D. Myers and W.J. Swiatecki, At. Data and Nucl. Data Tables 59 (1995) 185.
[17] E. Rost, Phys. Lett. B 26 (1968) 184.
[18] A. Chepurnov, Yad. Fiz. 6 (1967) 955.
[19] J. Dudek, A. Majhofer, J.Skalski, T. Werner, S. Ćwiok and W. Nazarewicz, J. Phys. 65 (1979) 1379.
[20] D. Vautherin, Phys. Rev. C 7 (1973) 296.
[21] M. Beiner, H. Flocard, Nguyen van Giai and P. Quentin, Nucl. Phys. A 238 (1975) 29.
[22] M.J. Giannoni and P. Quentin, Phys. Rev. C 21 (1980) 2076.
[23] J. Bartel, P. Quentin, M. Brack, C. Guet and H.-B. Høakanson, Nucl. Phys. A 386 (1982) 79.
[24] S. Köhler, Nucl. Phys. A 258 (1976) 301.
[25] J. Dobaczewski, H. Flocard and J. Treiner, Nucl. Phys. A 422 (1983) 103.
[26] P. Ring, Prog. Part. Nucl. Phys. 37 (1996) 193.
[27] G.A. Lalazissis, J. König and P. Ring, Phys. Rev. C 55 (1997) 540.
[28] P.G. Reinhard, M. Rufa, J. Mahrun, W. Greiner and J. Friedrich, Z. Phys. A 323 (1986) 13.
[29] M.M. Sharma, M.A. Nagarajan and P. Ring, Phys. Lett. 312 (1993) 377.
[30] Y.K. Gambhir, P. Ring and T. Thimet, Ann. Phys. 198 (1990) 132.
[31] G. Audi and A.H. Wapstra, Nucl. Phys. A 565 (1993) 1.
[32] B. Nerlo-Pomorska and K. Pomorski, Z. Phys. A 348 (1994) 169.
[33] W. Bertozzi, J. Friar, J. Heisenberg and J.W. Negele, Phys. Lett. B 41 (1972) 408.
[34] M. Nishimura and D.W.L. Sprung, Prog. Theor. Phys. 77 (1987) 781.
[35] R.W. Hasse and W.D. Myers, Geometrical Relationships of Macroscopic Nuclear Physics (Springer, 1988).
[36] H. de Vries, C.W. de Jager and C. de Vries, At. Data and Nucl. Data Tables 36 (1987) 495.
[37] E.W. Otten, *in* Treatise on heavy-ion science, Vol .8, ed. D.A. Bromley (Plenum, New York, 1989) p. 517.
[38] B. Nerlo-Pomorska and B. Mach, At. Data and Nucl. Data Tables 60 (1995) 287.
[39] A. Baran, L. Egido, B. Nerlo-Pomorska, K. Pomorski, P. Ring and L.M. Robledo, J. Phys. C 21 (1995) 657.
[40] A. Baran, W. Höhenberger, Phys. Rev. 153 (1996) 1570.